Agriculture, Ecosystems and Environment 251 (2018) 26–36

Contents lists available at ScienceDirect

Agriculture, Ecosystems and Environment

journal homepage: www.elsevier.com/locate/agee

Research paper

The dynamic mechanism of landscape structure change of arable landscape system in China

Penghui Jiang[a,b], Qianwen Cheng[a,b], Zhuzhou Zhuang[a,b], Haoqing Tang[a,b], Manchun Li[a,b,c,*], Liang Cheng[a,b,c,**], Xiaolong Jin[a,b]

[a] School of Geographic and Oceanographic Sciences, Nanjing University, Nanjing 210023, China
[b] Jiangsu Provincial Key Laboratory of Geographic Information Science and Technology, Nanjing University, Nanjing, 210093, China
[c] Collaborative Innovation Center for the South Sea Studies, Nanjing University, Nanjing 210093, China

ARTICLE INFO

Keywords:
Climatic characteristics difference
Urban expansion
Population mobility
Arable landscape system classification
Geographically weighted regression (GWR)
Redundancy analysis (RDA)

ABSTRACT

The healthy functioning of arable landscape ecosystems depends on their functional structure and productivity. In view of current global climate change and constant population mobility, the global agricultural industry has to address the effects of such factors on the functional structure of arable lands. In our research on these issues, we combined information on land use/cover changes with several other datasets. These include meteorological data from 1 823 national and local meteorological stations, agrometeorological disasters from 430 national monitoring stations, and population surveys covering 9 856 townships. Our findings indicate that the arable landscape system in China shows an overall trend of fragmentation, with the extent of the core arable land decreasing by 10 336.06 km^2. This trend is affected minimally by climate differences and population changes in traditional agricultural regions. However, in eastern and western China, the trend is affected significantly by the rate of population aging, the population migration rate, and the agricultural labor scale. Urban land expansion plays a key role in changing the arable landscape system. Rapid urbanization in the form of an integral transition from arable land to construction, which is represented by large-scale increase in construction land area, is the core dynamic mechanism of landscape structure change of arable landscape systems in China.

1. Introduction

Arable lands are vital resources that play a significant role in the survival of the human species. In addition, such land resources form the basis for economic development and social stability, and constitute an important component of national security (Kastner et al., 2014). In recent years, the worldwide extent of arable land has shown a decreasing trend that is attributable to various factors, including social and economic development, the effects of natural disasters, warfare, and system reforms. Accordingly, the quality of arable lands has declined correspondingly (Foley et al., 2011; Renwick et al., 2013; Deng et al., 2015; Pribadi and Pauleit 2015; Song et al., 2015), and the agricultural production potential of various major food-exporting countries has been reduced (Zumkehr and Campbell, 2015). To compound matters, the continuous growth of the population is placing increasing pressure on global food supplies, exacerbating the food security problem (Godfray et al., 2010; Zumkehr and Campbell, 2015). Moreover, studies have indicated that the global demand for food will double by 2050, adding to the international concerns about food security (Green et al., 2005).

In this regard, China, in view of its vast population, is hard pressed to ensure national food security. In fact, food security is a critical condition for maintaining peace and stability nationally as well as internationally. The basis for ensuring food security in China and elsewhere is to protect the quality of arable lands and to pursue continuous improvement in the productivity of such land resources (Kong, 2014). Currently, the main threats to the sustainable use of arable lands in China include such lands being taken over for other uses because of urban sprawl and development, and changes to the natural environment arising from climate change (Piao et al., 2010; Song et al., 2015). The former problem has already been contained to a certain extent by the introduction of a series of policies to protect and preserve arable lands. However, the latter issue is likely to persist and, in the medium to long term, would probably have the most significant effect on arable lands in the country (Reidsma et al., 2010; Huang and Wang, 2014; Tendall and Gaillard, 2015; Narges et al., 2016)

* Corresponding authors at: School of Geographic and Oceanographic Sciences, Nanjing University, Nanjing 210023, China.
** Corresponding author at: School of Geographic and Oceanographic Sciences, Nanjing University, Nanjing 210023, China.
E-mail addresses: jiangph1986@163.com (P. Jiang), chengqw1992@163.com (Q. Cheng), zhuangzhuzhou@163.com (Z. Zhuang), dz1627005@smail.nju.edu.cn (H. Tang), manchun@nju.edu.cn (M. Li), lcheng@nju.edu.cn (L. Cheng), 157512204@qq.com (X. Jin).

http://dx.doi.org/10.1016/j.agee.2017.09.006
Received 29 April 2017; Received in revised form 1 September 2017; Accepted 12 September 2017
Available online 28 September 2017

The effects of climate change and socio-economic development on arable lands have become matters of global concern (Alexander et al., 2015; Narges et al., 2016). Research has enriched our understanding of the relationship between climate change and agricultural and economic development (Dall'erba and Domínguez, 2015; Mathilde et al., 2015) as well as our knowledge of the effects of climate change on agricultural production (Lobell et al., 2012; Cynthia et al., 2014; Delphine et al., 2016). The consensus is that climate change threatens both the steady rate of agricultural production and attempts to increase food supplies (Tao et al., 2009; Xiong et al., 2009; Piao et al., 2010; Zhang et al., 2011). However, several aspects require further study (Cynthia et al., 2014), such as the effects of system changes in arable landscapes and the driving factors of these changes, which, to date, have not been explained fully (Narges et al., 2016). Recent studies on such aspects employed data from diverse sources, and mostly focused on the effects of climate change on crop yields by employing statistical computations, model simulations, or the inversion of remote sensing data (Tao et al., 2009; Lobell et al., 2012; Mu et al., 2012; Cynthia et al., 2014). Nonetheless, other factors have been neglected, such as the effects that differences in climate characteristics and population mobility have on system changes in arable landscapes that inevitably lead to a decrease in the productivity of these arable lands.

Accordingly, this study attempted to fill these gaps from a new perspective, i.e., by proposing a classification model of arable landscape systems (ALS). The aim was to address the following questions: (i) What is the spatial change law and tendency of Chinese ALS? (ii) Regarding trends in the spatiotemporal evolution of ALS types in China and the response mechanism of ALS to climate differences, population changes, and urban expansion, can ALS changes be explained adequately by these factors? (iii) What is the dynamic mechanism of the core driving forces of changes in ALS.

2. Methods

2.1. Classification model for ALS types

According to the geographic law of attenuation with distance and the theory of edge effects in landscape ecology, the ecological functions of a particular geographic landscape unit are closely related to its spatial location. Regarding an ALS, the farther it is located from the core of that system the less stable it would be, and vice versa. Lands for cultivation located between arable and non-arable lands are extremely vulnerable to the effects of non-agricultural activities occurring at the peripheries. Consequently, such lands have distinct production or ecological functions from lands located at the core of the ALS. Similarly, if a tract of land for cultivation is located in isolation at the core of an arable landscape system and is spatially surrounded by non-agricultural landscapes, it does not have the conditions for stable agricultural production. This is because it lacks the appropriate agricultural background and environment.

Based on the aforementioned theories and the findings of related studies (Vogt et al., 2007; Riitters et al., 2009; Cheng et al., 2015a,b), the current study applied the mathematical morphology pattern recognition method to distinguish various ALS types. This application led to the definition of four types of arable land (Fig. S1):

(i) *Core arable lands*: These are spatially isolated from non-arable landscapes and are internally formed by homogeneous and contiguous arable lands. Such lands constitute the basic environment that helps maintain arable land ecosystems and stable production. The scale of core arable lands in a region directly determines the agricultural production ability and potential of such a region.
(ii) *Edge arable lands*: These lands coexist with core arable lands and are spatially distributed at the peripheries of the former. Such lands serve as the buffer or transition zone between arable and non-arable lands and are different from the complex core–edge environments that exist within core arable lands. Edge arable lands reflect the effects of external non-agricultural uses on arable land ecosystems. Increases in the number of such lands reflect the increasing magnitudes of the decrease of core arable lands.
(iii) *Perforated arable lands*: These lands are surrounded spatially by core arable lands, but are also adjacent to non-arable lands. The scale of this category of arable lands is indicative of the degree of erosion that is occurring within the core ALS. Increases in the scale of such lands accelerate the rate at which the structure of core ALS disintegrates.
(iv) *Patch arable lands*: In terms of distribution, these lands are isolated from core arable lands and surrounded by non-agricultural environments. The size of their internal habitat area is small and they do not contain any core–edge environments. They reflect the extent of fragmentation that the regional arable landscape is subject to and when such lands become the predominant arable landscape, it indicates that the overall arable landscape of a region has become fragmented.

Subsequently, we employed land use/cover data of China for the 1980s, 1995, 2000, 2005, and 2010 as the base data (resolution: 1 km; The data set is provided by Data Center for Resources and Environmental Sciences, Chinese Academy of Sciences (RESDC) (http://www.resdc.cn)). The aforementioned classification of arable lands and the relationship between four adjacent domains were used as reference for the spatial identification of ALS as well as to design the following classification method:

(i) *Classification of core arable lands*: If the central and peripheral pixels within the structure of four adjacent domains were all arable lands, the central pixel would be core arable land. The algorithm design is shown in Fig. S2.
(ii) *Classification of perforated arable lands*: Depending on the classification result of core arable lands, a hole-filling algorithm was performed to fill the internal voids of core arable lands. Subsequently, the arable land pixels similarly coexisting with core arable lands and spatially located in the ALS and adjacent to any non-arable lands were defined as perforated arable lands. In the spatial structure of adjacent domains, perforated arable lands are located in an intermediate position between non-arable and core arable lands. The algorithm design is shown in Fig. S3.
(iii) *Classification of edge arable lands*: Similar to the classification of perforated arable lands, edge arable lands were classified based on core arable lands. Through a morphological dilation on core arable lands and the exclusion of core and perforated arable and non-arable lands, edge arable lands were classified as peripheral arable land pixels of core arable lands. The algorithm design is shown in Fig. S4.
(iv) *Classification of patch arable lands*: These lands are surrounded by non-arable landscapes and are spatially isolated from the core arable lands. In the structure of the adjacent domains, patch arable lands have only an adjacency relationship with edge arable lands, non-arable lands, or other similar patch arable lands. Therefore, after the core, edge, and perforated arable lands were determined, all the remaining pixels for arable lands could be uniformly classified as patch arable lands. The algorithm design is shown in Fig. S5.

2.2. Process of change between ALS types

The Markov chain transition matrix was used to analyze the process of dynamic changes in the arable lands and their landscape structures in China. This matrix can show information on the dynamic processes of the mutual transitions between ALS types that occur between the beginning and end of a specific period (Hill et al., 2002; Solow and Smith, 2006). The theoretical concept can be expressed as follows:

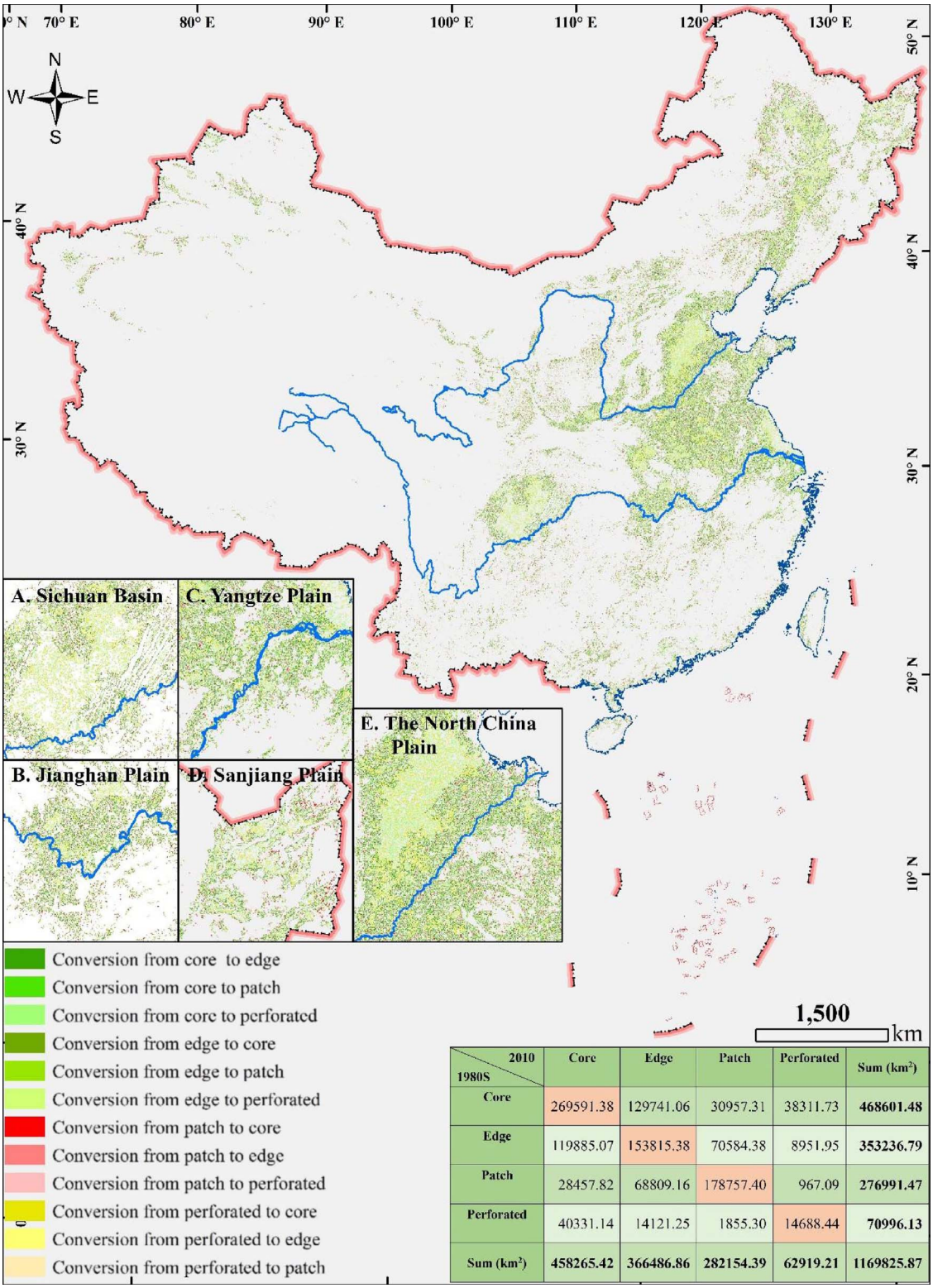

1980S \ 2010	Core	Edge	Patch	Perforated	Sum (km²)
Core	269591.38	129741.06	30957.31	38311.73	**468601.48**
Edge	119885.07	153815.38	70584.38	8951.95	**353236.79**
Patch	28457.82	68809.16	178757.40	967.09	**276991.47**
Perforated	40331.14	14121.25	1855.30	14688.44	**70996.13**
Sum (km²)	**458265.42**	**366486.86**	**282154.39**	**62919.21**	**1169825.87**

Fig. 1. Spatial changes in arable landscape systems of China during 1980–2010. A–E show the major grain production areas, and the table shows the conversion scale between different arable landscape types.

$$A_{ij} = \begin{bmatrix} A_{11} & \dots & A_{1n} \\ \vdots & \vdots & \vdots \\ A_{n1} & \dots & A_{nn} \end{bmatrix}$$

Where A is land area; n represents the number of ALS types before and after the transition; i and j represent the specific ALS type before and after transition, respectively; and A_{ij} indicates the area of ALS type i that became ALS type j during the transition.

Each row of elements in the matrix represents the information flow of ALS type i as it transitioned to other ALS types. Each column of elements in the matrix represents the information source of various ALS types before they transitioned to areas of ALS type j.

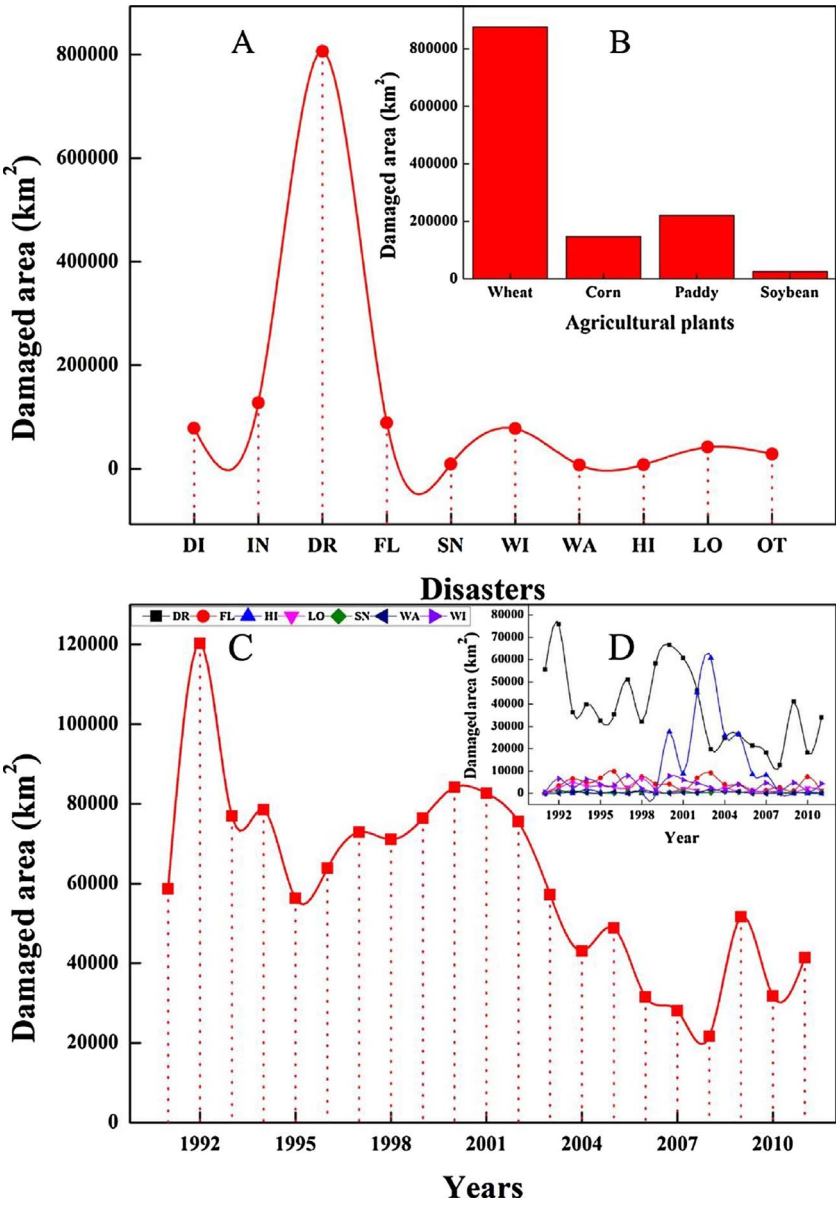

Fig. 2. Damage scale of agricultural land in China resulting from meteorological and non-meteorological disasters during 1991–2011. A shows the cumulative damage scale of agricultural land resulting from crop disease (DI), insects (IN), drought (DR), floods, rainstorms, and continuous rainfall (FL), snow and hailstones (SN), wind (WI), waterlogging (WA), high temperatures (HI), low temperatures (LO), and other agriculture disasters (OT); B shows the cumulative damage scale of different agricultural plants; C shows the temporal change of the damage scale of arable land in China from 1991 to 2011; D shows to the temporal changes of the damage scale resulting from different disasters from 1991 to 2011.

2.3. Ordination analysis model

We explored the interrelationship between the function structure and productivity of arable land and climate differences and population change by using the area of lands affected by ALS changes and the productivity of arable land (represented by crop yields) as dependent variables, with the various climatic factors as independent variables. The purpose was to explore the relationship between changes in the climate and environment as well as the spatial variations in both ALS and the productivity of ALS.

Building of the sorting model involved the following steps:

(i) *Sample selection*: The meteorological station was the starting point for building the model for climate differences and ALS changes, with a 10 km radius around it designated as the buffer zone for analysis. The monitoring data from the meteorological station were treated as independent variables for that buffer zone, whereas changes in the ALS areas were considered the dependent variables (Fig. S6). Model building for population and ALS changes was based on the administrative zones of the town. In order to reflect the socio-economic differences among east, central, and west China and the natural differences between north and south China, two transects were set to construct the analysis model (Fig. S7). While building the model for climate differences and productivity changes of arable lands, the starting point was the monitoring site for crop yields (with its data treated as dependent variables). First, each crop-yield monitoring site was matched with a local meteorological station. If none were available, distance analysis was performed to select the closest meteorological station. Subsequently, data from the matching meteorological station were treated as independent variables (Fig. S8).

(ii) *Selection of optimal model*: Detrended correspondence analysis (DCA) was conducted on the dependent variables to select the optimal model for sorting analysis. If the maximum value for the length of a gradient in the analysis results was greater than 4.0, canonical correlation analysis (CCA) was chosen. If the value was 3.0–4.0, either CCA or redundancy analysis (RDA) could be selected. If the value was less than 3.0, the results from RDA were superior to those from CCA. Based on the DCA results (Tables S1 and S2), the RDA model was selected for this study. The RDA model is a direct sorting model that searches for potential or indirect environmental gradients to explain changes in species data.

Table 1
Contributions of differences in climatic characteristics to spatial pattern changes in arable land in China.

a. Relation between core farmland change and climatic characteristics difference

Axes	1	2	3	4	Total variance
Eigenvalues	0.090	0.016	0.003	0.000	1.000
Species-environment correlations	0.550	0.182	0.236	0.259	
Cumulative percentage variance of species data	9.200	6.300	6.600	6.600	
Cumulative percentage variance of species-environment relation	73.80	95.40	99.90	100.0	
Sum of all eigenvalues	1.000				
Sum of all canonical eigenvalues	**0.125**				

b. Relation between edge farmland change and climatic characteristics difference

Axes	1	2	3	4	Total variance
Eigenvalues	0.090	0.030	0.010	0.000	1.000
Species-environment correlations	0.420	0.290	0.300	0.240	
Cumulative percentage variance of species data	9.200	12.40	13.20	13.30	
Cumulative percentage variance of species-environment relation	69.30	93.20	99.40	100.00	
Sum of all eigenvalues	1.000				
Sum of all canonical eigenvalues	**0.133**				

c. Relation between patch farmland change and climatic characteristics difference

Axes	1	2	3	4	Total variance
Eigenvalues	0.160	0.050	0.020	0.000	1.000
Species-environment correlations	0.470	0.500	0.520	0.340	
Cumulative percentage variance of species data	16.20	21.30	23.10	23.10	
Cumulative percentage variance of species-environment relation	70.20	92.20	99.80	100.00	
Sum of all eigenvalues	1.000				
Sum of all canonical eigenvalues	**0.231**				

d. Relation between perforated farmland change and climatic characteristics difference

Axes	1	2	3	4	Total variance
Eigenvalues	0.080	0.050	0.020	0.000	1.000
Species-environment correlations	0.430	0.380	0.260	0.330	
Cumulative percentage variance of species data	8.200	12.70	14.20	14.30	
Cumulative percentage variance of species-environment relation	57.10	88.40	99.10	100.00	
Sum of all eigenvalues	1.000				
Sum of all canonical eigenvalues	**0.143**				

(iii) *Model computations*: This model mainly used CANOCO 4.5 for analysis, which is international standard generic software (Terbraak and Smilauer, 2002). The actual technology roadmap is shown in Fig. S9.

2.4. Land development intensity

Land development intensity (LDI) reflects the scale and frequency of human effects on land cover and land use change (Liu et al., 2013). It can be explained as the ratio of artificial land cover area in a certain region. In this study, we selected construction land as the major land use type to reflect human development activities. Subsequently, the ratio of construction land area was used to calculate the LDI in a certain region. The formula for LDI is as follows:

$$LDI = \frac{CA}{TA} \times 100\%$$

Where *CA* refers to the construction land area in a certain computation area (grid or administrative cell), and *TA* refers to the total area of the certain computation area (grid or administrative cell).

2.5. Dynamic degree of land use

Land use dynamic degree (LUDD) is used to reflect the change of land use in telophase relative to the initial time (Liu et al., 2010). It involves two concepts, namely a single and a comprehensive dynamic degree. The former is used to reflect the change of single land use types, whereas the latter can reflect the variation of different land use and land cover changes. In this study, we selected the single dynamic degree to reflect changes in ALS. The single dynamic degree was calculated as follows:

$$LUDD = \frac{(A_i - A_j)}{A_j} \times 100\%$$

Where A_i refers to the area of a certain land use type at the initial time, and A_j refers to the area of such a land use type at the telophase time.

2.6. Geographically weighted regression model

Land use and land cover change varies in different regions because of geographical spatial heterogeneity. Traditional regression analyses have limitations in reflecting spatial constrains, whereas the geographically weighted regression (GWR) model can overcome such a problem by considering locations (Fotheringham et al., 2002; Charlton et al., 2009). The GWR model is a local linear regression method that can model spatially varying relationships of different geographical phenomena (Fotheringham et al., 2002).

Since the spatial expression forms of climate and population data are different with arable land, it is difficult to construct the GWR relationship with a suitable sample method. In contrast, arable and urban land can be significantly correlated spatially. Therefore, we selected the GWR model to explore the dynamic mechanism between urban land change and variations of ALS. The LDI of a county was defined as an explanatory variable and the LUDD of different arable landscape types was defined as the dependent variable. The equation for the GWR model in this study was as follows:

$$LUDD_x = k + \alpha_1 \times LDI + \varepsilon_1$$

Where $LUDD_x$ refers to the dynamic degree of arable landscape types x, α_1 refers to the intercept value, and ε_1 refers to the model residual. The model was performed by using ArcGIS 10.2 software, and related procedures are referenced the help of ArcGIS software.

3. Data

We utilized accurate monitoring data on land use/cover changes in China over five time periods (1980s, 1990, 1995, 2000, 2005, and 2010, The data set is provided by Data Center for Resources and Environmental Sciences, Chinese Academy of Sciences (RESDC) (http://www.resdc.cn)), meteorological data from 1 823 national and local meteorological stations (1981–2010) (listed in Data 1, http://data.cma.cn/), data on agrometeorological disasters from 430 national monitoring stations (1991–2011) (listed in Data 2, http://data.cma.cn/), and population survey data covering 1 491 townships (2000, 2010) (listed in Data 3, http://www.stats.gov.cn/).

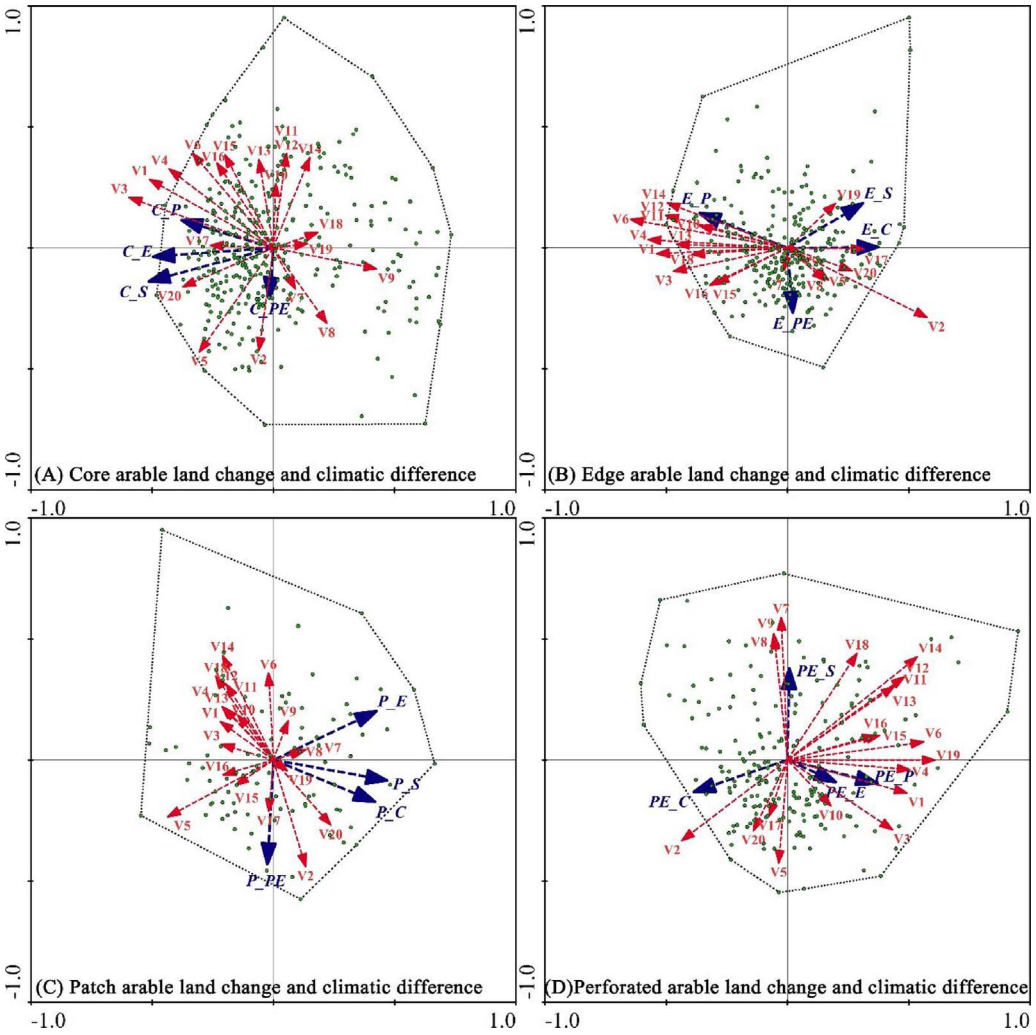

Fig. 3. Gradient ordination between climate factors (red font and arrows) and arable landscape pattern change (blue font and arrows). (For interpretation of the references to colour in this figure legend, the reader is referred to the web version of this article.)
V1: annual mean temperature (normal); V2: daily range of annual mean temperature (normal); V3: annual mean maximum temperature (normal); V4: annual mean minimum temperature (normal); V5: annual extreme maximum temperature (normal); V6: annual extreme minimum temperature (normal); V7: relative mean difference in annual temperature (normal): V8: standard deviation in annual temperature (normal); V9: maximum positive anomaly in annual mean temperature (normal); V10: maximum negative anomaly in annual mean temperature (normal); V11: annual average precipitation at 20:00 (normal); V12: annual average precipitation at 08:00 (normal); V13: annual maximum precipitation (normal); V14: annual minimum precipitation (normal); V15: relative mean difference in annual precipitation (normal); V16: standard deviation in annual precipitation (normal); V17: maximum percentage of positive anomalies for annual precipitation (normal); V18: maximum percentage of negative anomalies for annual precipitation (normal); V19: month with maximum number of consecutive wet days (normal); V20: month with maximum number of consecutive dry days (normal).

4. Results and discussion

4.1. Spatiotemporal evolution of landscape structures of China's arable lands

The landscape structures of arable lands in China could be categorized generally into contiguous core arable lands and dispersed patch arable lands, which represented more than 60% of the arable land resources of China (Fig. 1). However, the significant overlap between core arable land and urban space changed this pattern (Liu, 2005, 2010; Cheng et al., 2015a,b). This overlap was attributed to rapid urbanization and development and the consequent intense competition for water, power, and human and other resources following the economic reforms in China during the 1980s. As a result, pronounced conflicts have developed between the need to preserve arable lands and the pressure to convert such lands for other land uses (Cheng et al., 2015a,b). At an aggregate level, the traditional landscape structures and patterns have remained relatively stable from the 1980s to 2010; however, the actual area of the various landscape structures has been subject to substantial changes (Fig. 1).

Over the years, the actual areas of core and perforated arable lands have declined by 10 336.06 km^2 and 8 076.92 km^2, respectively (Fig. 1). In contrast, the areas consisting of patch and edge arable lands have increased by 5 162.91 km^2 and 13 250.06 km^2, respectively (Fig. 1). The reduction in the proportion of core arable lands, combined with the increase in patch arable lands, point to a trend of fragmentation of arable landscapes in China. On the other hand, an increase in the proportion of edge arable lands and a reduction in perforated arable lands show that (i) erosion of fringe areas by non-agricultural activities remains the main mechanism through which the arable lands are being fragmented, and (ii) the external expansion of core arable lands through perforation has been reduced progressively. The predominant result of the evolution of landscape structures was the conversion of core arable lands to other types of arable lands.

At the macro level, the fragmentation of core arable lands has increasingly become the main mechanism for ALS changes. This is applicable to the following areas: (i) Sichuan Basin, where the Chengdu metropolitan area is located (Fig. 1A), (ii) Jianghan Plain, where the Wuhan metropolitan area is located (Fig. 1B), (iii) the middle and lower reaches of the Yangtze River Basin, which is the location of the Yangtze River Delta metropolitan area (Fig. 1C), (iv) North China Plain, which is the location of the Beijing-Tianjin-Hebei metropolitan area (Fig. 1D), and (v) the Sanjiang Plain, the most important production base for commercial food crops in China (Fig. 1E). However, this trend of fragmentation of arable landscapes at the macro level has been effectively curbed since the promulgation of the *Regulations on the Protection of Basic Arable Land* by the Chinese government in 1998 (Lichtenberg and Ding, 2008; Cheng et al., 2015a,b). Consequently, conversions between various ALS types have decreased significantly in the decade 2000–2010 (Fig. S10).

However, policy change only cannot fully explain the changes in ALS at a macro level. The beginning of ALS change is not a sudden phenomenon but a complex process with a series of human activities and natural effects, especially for China, a country characterized by

Table 2
Geographically weighted regression model analysis of land development intensity (LDI) and arable land system change in China.

Varname	Variable11	Definition 1	Variable12	Definition 2
Band width	332271.09		332271.09	
Residual Squares	3.01		16.56	
Effective Number	45.20		45.20	
Sigma	0.06		0.15	
AICc	−1991.99		−688.48	
R^2	0.49		0.43	
R^2 Adjusted	0.46		0.39	
Dependent Field	0.00	ALDD	0.00	CALDD
Explanatory Field	1.00	LDI	1.00	LDI

Varname	Variable13	Definition 3	Variable14	Definition 4
Band width	46822173.34		46822173.34	
Residual Squares	6686.14		13384.15	
Effective Number	2.01		2.01	
Sigma	2.96		4.19	
AICc	3835.47		4366.40	
R^2	0.01		0.01	
R^2 Adjusted	0.01		0.01	
Dependent Field	0.00	EALDD	0.00	PALDD
Explanatory Field	1.00	LDI	1.00	LDI

Varname	Variable15	Definition 5
Band width	46822173.34	
Residual Squares	7097511.27	
Effective Number	2.01	
Sigma	96.45	
AICc	9165.58	
R^2	0.00	
R^2 Adjusted	0.00	
Dependent Field	0.00	PEALDD
Explanatory Field	1.00	LDI

Notes: ALDD→ Dynamic degree of arable land; CALDD→ Dynamic degree of core arable land; EALDD→ Dynamic degree of edge arable land; PALDD→ Dynamic degree of patch arable land; PALDD→ Dynamic degree of perforated arable land; Sample numbers→ 765

significant landscape heterogeneity. Since more than 80% of arable lands in China are concentrated in the eastern parts of the population line and monsoon areas, and overlaps with urban lands, we put forward the hypothesis that the major driving forces of ALS change are climate, population, and urban land expansion. However, the dynamic mechanism of how climate, population, and urban land expansion affect the process of ALS change still needs further exploration.

4.2. Effects of climate on ALS

Climatic factors, such as temperature, precipitation and humidity, are crucial to agricultural crops, which makes climate an important natural driver for the formation and development of ALS. Plains with appropriate climatic conditions are easily to be continuously ALS. In contrast, ALS under poor hydrothermal conditions are mostly fragmented because of the growth restrictions of agriculture crops. In many cases, the effects of climate on ALS depend on climatic differences and meteorological disasters.

4.2.1. Effects of agrometeorological disasters on ALS

Agrometeorological disasters are a direct effect of climate change influencing agricultural landscapes. Agricultural disasters include those caused by crop diseases and pests as well as damage caused by droughts, floods, frost, and cold. Agrometeorological disasters constitute the main effects of climate differences on ALS in China (Zhang et al., 2014a,b; Wang et al., 2016). In addition, we noticed high degrees of fit between the spatial distribution of various types of meteorological disasters (including droughts, floods and waterlogging, windstorms, snowstorms, and frost and cold damage) and that of arable lands. These arable lands are located in temperate, subtropical, tropical, and other climate zones as well as in regions with mountains, plateaus, plains, basins, and other geomorphic features. In contrast, disasters related to heat damage were concentrated in the southern regions of China, and were generally consistent with the crop-growing seasons and the spatial distribution characteristics of temperatures in China. This finding further indicates the close relationship between agrometeorological disasters and the productivity of arable land ecosystems. In terms of scale, the cumulative hazard land area in China caused by droughts alone during 1991–2011 amounted to more than 806 402.00 km^2 (Fig. 2A), accounting for 63.38% of the total cumulative hazard land area affecting the agricultural industry over the same period. On the other hand, the combined proportion of cumulative hazard land area caused by crop diseases and pests as well as non-meteorological disasters amounted to approximately 18.95% (Fig. 2A). Over various periods during 1991–2011, the cumulative hazard land area caused by droughts almost completely exceeded that caused by other types of meteorological disasters (with the exception of heat damage) and non-meteorological disasters (Fig. 2D).

Among the various crops cultivated in China, wheat was most affected by meteorological disasters in terms of hazard land area (Fig. 2B). The cumulative hazard land area for wheat during 1991–2011 was as much as 876 409.33 km^2, accounting for 68.88% of the total hazard land area affecting the four major crops for which statistics were compiled. This indicates that differences in climate characteristics are significant factors determining fluctuations in wheat yields (Godfray et al., 2011; Zhang et al., 2014a,b). Separately, the land areas of various crop types affected by drought and precipitation far exceeded those caused by other types of meteorological disasters (Figs. 2A and D). This shows that temperature and precipitation are the most important climatic factors that affect the ALS in China.

However, it should be noted that the magnitude of crops affected during 1991–2011 showed a trend of gradual decline, with the trend of the effect of climate differences on ALS also declining. This could be ascribed to the increased resilience of ALS to disasters, attributable to increasingly advanced agrotechnologies (such as research and development on seeds of drought-resistant crops and drip-irrigation technologies) and the construction of large-scale water-conservation facilities (such as the South-to-North Water Diversion Project and the Three Gorges Dam in China). These advances show that the progress of human civilization is able to ameliorate the effects of climate differences on arable landscapes.

4.2.2. Effects of climatic characteristics differences on evolution of ALS types

Regional climate is a fundamental natural condition that affects arable lands (Cohn et al., 2016). Long-term fluctuations and variations in crucial climatic factors, such as sunlight, heat, and precipitation pose certain constraints on the spatiotemporal evolution of arable landscapes (Cohn et al., 2016). However, in the short term, climate differences did not affect arable landscapes significantly, specifically not large areas of contiguous arable lands. Research has shown that climate differences account for only 12.5%, 13.3%, and 14.3% of total changes to core, edge, and perforated arable lands (Table 1a, b, and d), respectively. This proves that at short temporal scales, climate differences have no significant effects on the main functional area of arable lands. In contrast, the habitat areas of patch arable lands are small and constantly being disturbed by various types of non-agricultural activities or uses. Therefore, climate differences strengthened the effects of such interferences to some extent. In particular, climate differences caused 23.1% of the total changes in patch arable lands (Table 1c). As core, edge, and perforated arable lands all have continuous landscape patterns and large habitat areas compared with patch arable lands, the interpretation ratios show that arable landscapes with larger habitat areas and a continuous patterns have greater resistance to the effects of climatic

Table 3
Contributions of population changes to the spatial pattern changes in arable land in China.

Transect I

A. Beijing						B. Shandong					
Axes	**1**	**2**	**3**	**4**	***T***	**Axes**	**1**	**2**	**3**	**4**	***T***
a	**0.13**	**0.04**	**0.01**	**0.00**	1.00	***a***	**0.02**	**0.01**	**0.00**	**0.00**	1.00
b	0.52	0.38	0.25	0.17		***b***	0.26	0.19	0.10	0.07	
c	12.80	16.40	17.40	17.70		***c***	2.30	3.20	3.50	3.60	
d	72.10	92.70	98.10	100.00		***d***	63.10	90.40	97.80	99.90	
e	1.00					***e***	1.00				
f	**0.177**					***f***	**0.036**				
C. Henan						D. Ningxia					
Axes	**1**	**2**	**3**	**4**	***T***	**Axes**	**1**	**2**	**3**	**4**	***T***
a	**0.04**	**0.01**	**0.00**	**0.00**	1.00	***a***	**0.22**	**0.05**	**0.01**	**0.01**	1.00
b	0.31	0.16	0.13	0.04		***b***	0.66	0.52	0.27	0.16	
c	3.70	4.40	4.60	4.60		***c***	21.60	26.70	27.60	28.10	
d	79.80	94.80	99.60	100.00		***d***	76.70	95.10	98.30	100.00	
e	1.00					***e***	1.00				
f	**0.046**					***f***	**0.281**				

Transect II

E. Shanghai						F. Anhui					
Axes	**1**	**2**	**3**	**4**	***T***	**Axes**	**1**	**2**	**3**	**4**	***T***
a	**0.17**	**0.05**	**0.02**	**0.01**	1.00	***a***	**0.05**	**0.04**	**0.00**	**0.00**	1.00
b	0.60	0.47	0.30	0.30		***b***	0.40	0.34	0.18	0.06	
c	16.80	22.20	24.00	24.70		***c***	4.60	8.10	8.60	8.70	
d	68.30	89.80	97.20	100.00		***d***	53.40	93.70	98.90	100.00	
e	1.00					***e***	1.00				
f	**0.247**					***f***	**0.087**				
G. Hunan						H. Yunnan					
Axes	**1**	**2**	**3**	**4**	***T***	**Axes**	**1**	**2**	**3**	**4**	***T***
a	**0.04**	**0.02**	**0.00**	**0.00**	1.00	***a***	**0.06**	**0.02**	**0.01**	**0.00**	1.00
b	0.30	0.27	0.15	0.10		***b***	0.40	0.26	0.26	0.08	
c	3.60	5.10	5.60	5.80		***c***	6.20	7.80	9.00	9.10	
d	61.70	89.20	96.40	100.00		***d***	68.30	86.20	98.80	99.90	
e	1.00					***e***	1.00				
f	**0.058**					***f***	**0.091**				

Notes : *a*→ Eigenvalues; *b*→ Species-environment correlations; *c*→ Cumulative percentage variance of species data; *d*→ Cumulative percentage variance of species-environment relation; *e*→ Sum of all eigenvalues; *f*→ Sum of all canonical eigenvalues; *T*→ Total variance.

differences. Patch arable landscapes are characterized by a small habitat area and spatial dispersion, leading to greater vulnerability to disturbances from climatic factors. The ordination results (Fig. 3C) indicate that temperature was the main climatic factor in changes in patch arable landscapes, such as the cumulative annual maximum temperature (*V3*) and the cumulative annual extreme minimum temperature (*V6*).

4.3. Response of systems change in arable landscapes to human activities

Many studies have shown a significant correlation between human activities and arable land change (Martellozzo et al., 2015; Song et al., 2015; Pribadi et al., 2015). However, research has focused mostly on the effects of human activities on arable land scale or pattern change, but relationships between that and ALS changes are omitted in many cases. Therefore, learning more about the effects of human activities on ALS change is important in protecting arable land or coordinating relationships between the construction and food security sectors. Based on the hypothesis that ALS changes are mostly attributable to human activities, including population and urban land expansion, we attempted to explore the dynamic mechanism from the perspective of population structure change and land development intensity.

4.3.1. Response of systems change in arable landscape to land urbanization process

The StdResid having been generally less than 2.5 proves that there was no alignment phenomenon in the GWR model, and the model had an adequate confidence value (Fig. S11). The results of the GWR model show that arable land and core arable land can be explained by LDI. According to the R^2 adjusted value of the GWR model, approximately 46% of changes in arable land dynamic degree and 39% of changes in core arable land dynamic degree were attributable to LDI variations (Table 2). However, other changes in ALS, such as patch, edge and perforated arable lands, were not adequately explained by LDI. Since core arable land was the major type of ALS, we concluded that urban expansion reflected by LDI had a great influence on ALS change. This is in accord with the trend of land use change since the reform and opening-up of China.

In China, rapid urbanization processes corresponding with large-scale construction land expansion has become the major land use type during the past decades. Because of the high overlap between arable and construction land and the superior quality of the former, conversion from arable to construction land is the major urbanization model. The statistics show that the average annual conversion from arable to construction land in China was as high as 189 100 ha during 2004–2010 (MLR, 2004, 2005, 2006, 2007, 2008a, 2008b, 2010). Therefore, variations in arable land and core arable land are significantly affected by land development intensity.

Based on the definitions of every ALS type, edge, patch, and perforated arable land can indicate the effects of internal and external non-agriculture environments on ALS and core arable lands. Since edge, patch, and perforated arable lands showed little correlation with LDI, the influencing mechanism of urban expansion on ALS is not edge erosion, internal wedging, or segmentation but integral transition in China.

4.3.2. Response of systems change in arable landscape to population change

The interpolation ratios of population change to ALS evolution in

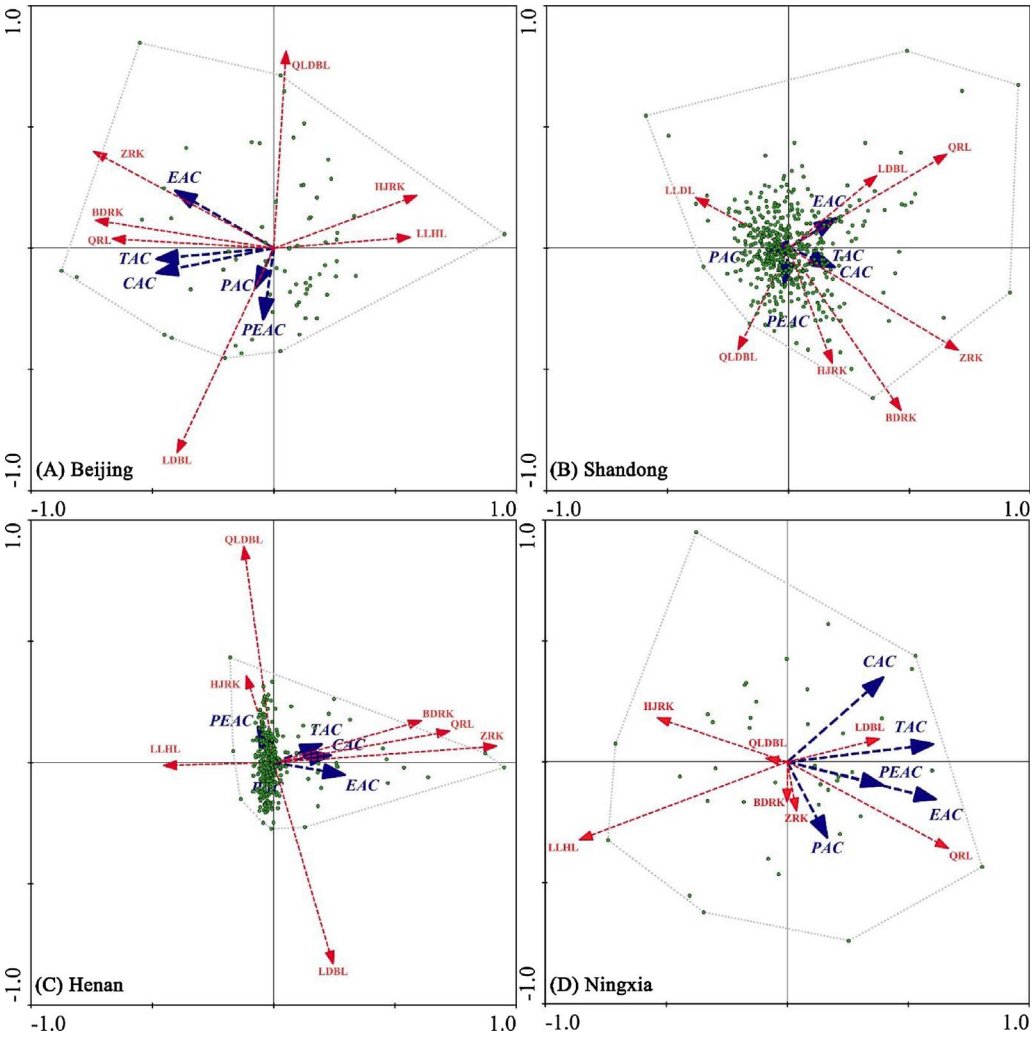

Fig. 4. Gradient ordination between population factors (red font and arrows) and arable landscape pattern change (blue font and arrows) of transect I. (For interpretation of the references to colour in this figure legend, the reader is referred to the web version of this article.)
BDRK: scale of native population; HJRK: population scale of each household; LDBL: proportion of labor population; LLHL: aging rate; QLDBL: potential rate of labor population; QRL: population migration rates; ZRK: total population scale.

transect I presented a U-shaped change in the gradient "Beijing → Shandong → Henan → Ningxia." Among these, the evolution of 17.70% and 28.10% in the ALS could be attributed to the population changes in Beijing and Ningxia, respectively (Table 3A and D). However, these ratios were only 3.60% and 4.60% in Shandong and Henan (Table 3B and C), respectively, which are traditional agricultural regions in China. In particular, the main population factors that cause changes in the ALS in Beijing are population migration rates, native population scale, aging rate, and the population scale of each household. The aging rate, particularly, is a driving force in system change in the arable landscape in Beijing. In Ningxia province, the population factors that drive such system changes are the labor population proportion and the aging rate. Similar to transect I, the interpolation ratio of population change to ALS evolution in transect II presents a U-shaped change in the gradient "Shanghai → Anhui → Hunan → Yunnan." In Shanghai, 24.70% of ALS evolution could be ascribed to population migration rates (Table 3E), potential labor population, and the population scale of each household. Elsewhere, such as in Anhui and Hunan provinces, only 8.70% and 5.80%, respectively, of changes were caused by population change (Table 3F and G).

The results of the model analysis show that population factors had more significant effects on changes in the ALS in east and west China, which are the traditional agricultural regions, compared with those in central China. Beijing and Shanghai are the more developed and advanced areas in China; therefore, they have been subject to sharp population declines in recent decades owing to the single-child policy. As a result, the aging and urbanization of the population have caused a rapid loss of the labor available for agriculture. Consequently, the agricultural development in these regions is dependent on population migration, i.e., people moving into these areas from elsewhere. Therefore, the main population factors responsible for changes in the ALS in east China were related positively to the migrant population and negatively to the rate of aging of the population (Figs. A and 5A). However, in west China, with a lower socio-economic development level, the large-scale emigration of the population and the labor-intensive irrigated agriculture, together with other factors, led to the agricultural labor scale being the most important population factor (Fig. 4D). In contrast, central China, with areas such as Shandong and Henan, and Anhui and Hunan provinces (Figs. Fig. 4B and C, Fig. 5B and C), was considered to have the highest population density and the most advanced agricultural science and technology. Consequently, the population contributed little to the changes in the ALS in these regions. Our findings match those of Lambin et al. (2013) and Godfray et al. (2011), who found close relationships between changes in land use methods and social factors, ecological trading, and policy.

5. Conclusions and policy recommendations

Using a classification model for arable landscapes, evaluation systems for the stability of productivity, and gradient analysis and respond analysis models for the dynamic mechanism of arable landscape change, we analyzed how ALS are affected by and respond to climatic differences and population change. We conclude that ALS in China show a trend of fragmentation. However, neither the differences in

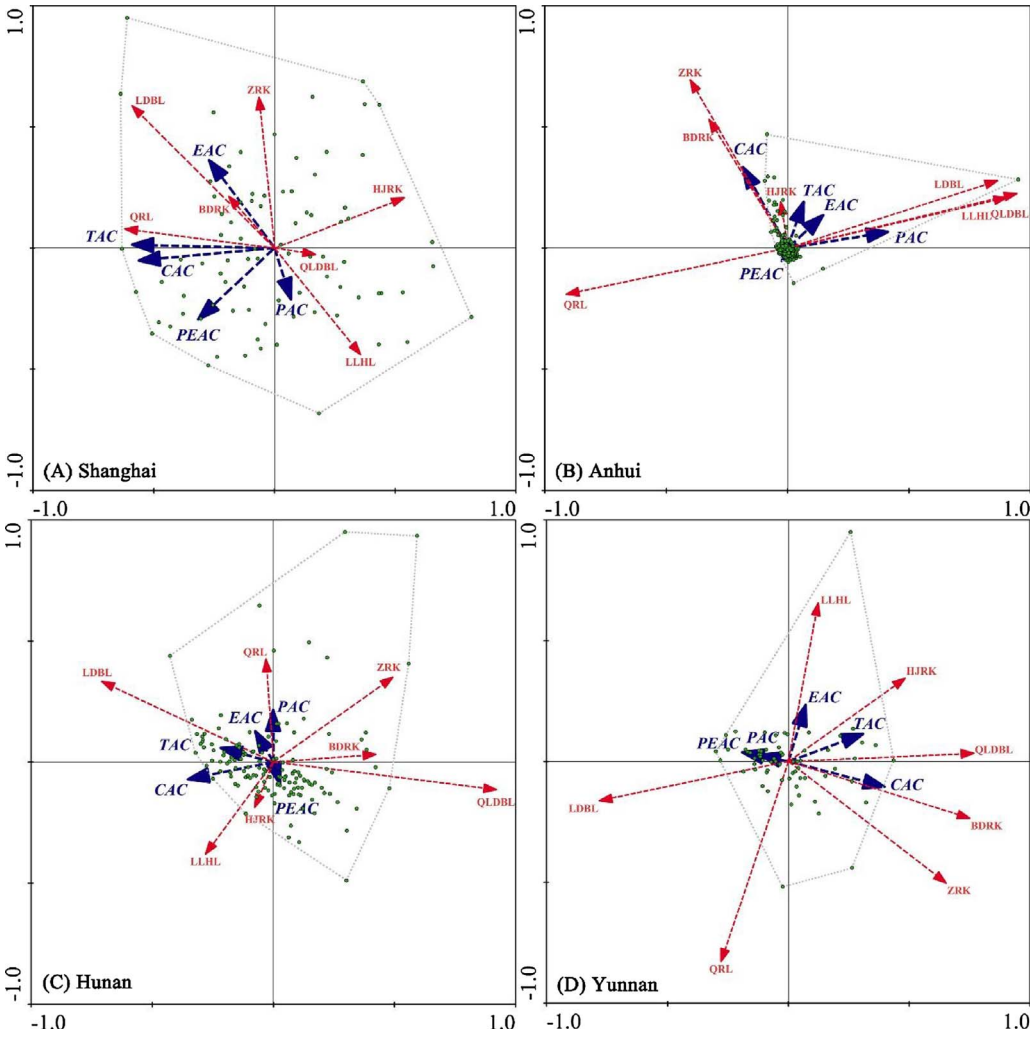

Fig. 5. Gradient ordination between population factors (red font and arrow) and arable landscape pattern change (blue font and arrow) of transect II. (For interpretation of the references to colour in this figure legend, the reader is referred to the web version of this article.)
BDRK: scale of native population; HJRK: population scale of each household; LDBL: proportion of labor population; LLHL: aging rate; QLDBL: potential rate of labor population; QRL: population migration rates; ZRK: total population scale.

climatic characteristics nor population mobility were able to adequately explain the changes in ALS in traditional agricultural regions. A continuous spatial pattern and larger habitat area can strengthen the resistance of ALS to various non-agricultural disturbances. Furthermore, the differences in climatic characteristics related to temperature fluctuations contributed significantly to the variations in the productivity of the arable land.

Currently, with large demands for grain products and land resources, China faces the dilemma of arable land protection and urban development because of large populations and overlap between arable lands and urban space. In order to solve such problems, it is necessary to construct two boundaries and two zones from the perspective of delineating the basic arable land protection area and urban development boundary. The two boundaries contain a flexible and rigid urban development boundary, which is used to constrain the scale and direction of urban sprawl. The two zones consist of basic farmland protection and flexible areas used in urban construction in the future, which are used to protect high-quality arable land and meet the demands of urban construction.

In summary, the following conclusions can be drawn: (i) Firstly, the productivity of arable land is highly related to its landscape structure. Core arable lands have the highest productivity because of the high continuity and little non-agricultural disturbance. Therefore, core arable land serves the main function of agricultural production in ALS. Subsequently, it is necessary to delineate the basic arable land protection area depending on the spatial distribution of core arable lands. Protection of core arable lands is the key to preventing a reduction in the productivity level of arable lands due to rapid urban expansion and frequent fluctuations in climatic conditions.

(ii) Moreover, rigid controlling of the scale and direction of urban sprawl must be insisted upon based on the needs of urban development. In China, urbanization is still the principal process of city development, and land demands will continuously increase. However, long-term inflation of urban scale and sprawl are detrimental to the ecological environment around city. Moreover, high-quality arable lands have experienced large-scale losses during the past decades. Therefore, two boundaries must be delineated to solve the conflict between urban development and restriction.

(iii) Since there is always a conflict between urban construction and arable land protection in China, it is necessary to coordinate such a relationship in the process of delineating the two boundaries and arable land protection zones. Consequently, a flexible area between urban space and arable land protection zones is needed to solve this conflict. The flexible area plays the role of ecological buffer zone to prevent urban pollutant diffusion and protect the core arable land from non-agricultural interference.

Acknowledgements

This work was supported by the National Key Research and Development Plan (Grant No. 2017YFB0504205), Program A for Outstanding PhD candidate of Nanjing University (No. 201602A011) and the Special Research Fund of the Ministry of Land and Resources for Non-Profit Sector (No. 201411014-03).

Appendix A. Supplementary data

Supplementary data associated with this article can be found, in the online version, at http://dx.doi.org/10.1016/j.agee.2017.09.006.

References

Alexander, P., et al., 2015. Drivers for global agricultural land use change: the nexus of diet, population, yield and bioenergy. Global Environ. Change 35, 138–147.

Charlton, M., Fotheringham, S., Brunsdon, C., 2009. Geographically weighted regression. White Paper. National Centre for Geocomputation. National University of Ireland Maynooth.

Cheng, L., et al., 2015a. Analysis of farmland fragmentation in China modernization demonstration zone since reform and openness: a case study of south jiangsu province. Sci. Rep. 5, 11797.

Cheng, L., et al., 2015b. Farmland protection policies and rapid urbanization in China: a case study for Changzhou City. Land Use Policy 48, 552–566.

Cohn, A.S., et al., 2016. Cropping frequency and area response to climate variability can exceed yield response. Nat. Clim. Change 6, 601–604.

Cynthia, R., et al., 2014. Assessing agricultural risks of climatic characteristics difference in the 21 st century in a global gridded crop model intercomparison. Proc. Natl. Acad. Sci. U. S. A. 111, 3268–3273.

Dall'erba, S., Domínguez, F., 2015. The impact of climatic characteristics difference on agriculture in the southwestern United States: the ricardian approach revisited. Spat. Eco. Anal. 11, 46–66.

Delphine, D., et al., 2016. Regional disparities in the beneficial effects of rising CO2 concentrations on crop water productivity. Nat. Clim. Change 6, 786–790.

Deng, X.Z., et al., 2015. Impact of urbanization on cultivated land changes in China. Land Use Policy 45, 1–7.

Foley, J.A., et al., 2011. Solutions for a cultivated planet. Nature 478, 337–342.

Fotheringham, A.S., et al., 2002. Geographically Weighted Regression: The Analysis of Spatially Varying Relationships. John Wiley & Sons Inc, Hoboken.

Godfray, H.C.J., et al., 2010. Food security: the challenge of feeding 9 billion people. Science 327, 812–818.

Godfray, H.C.J., et al., 2011. Linking policy on climate and food. Science 331 (331), 1013–1014.

Green, R.E., et al., 2005. Farming and the fate of wild nature. Science 307, 550–555.

Hill, M.F., et al., 2002. Spatio-temporal variation in Markov chain models of subtidal community succession. Ecol. Lett. 5, 665–675.

Huang, J., Wang, Y., 2014. Financing sustainable agriculture under climatic characteristics difference. J. Integr. Agric. 13, 698–712.

Kastner, T., et al., 2014. Rapid growth in agricultural trade: effects on global area efficiency and the role of management. Environ. Res. Lett. 9, 034015.

Kong, X.B., 2014. China must protect high-quality arable land. Nature 506, 7.

Lambin, E.F., et al., 2013. Estimating the world's potentially available cropland using a bottom-up approach. Global Environ. Change 23, 892–901.

Lichtenberg, E., Ding, C., 2008. Assessing farmland protection policy in China. Land Use Policy 25, 59–68.

Liu, J.Y., et al., 2010. Spatial patterns and driving forces of land use change in China during the early 21 st century. J Geogr. Sci. 20, 483–494.

Liu, M., Tao, Y., Li, D., et al., 2013. Exploring on urban land development intensity based on artificial neural network methods. JCP 8, 3119–3125.

Liu, J.Y., et al., 2005. Spatial and temporal patterns of China's cropland during 1990–2000: An analysis based on Landsat TM data. Remote Sens. Environ. 98, 442–456.

Lobell, D.B., et al., 2012. Extreme heat effects on wheat senescence in India. Nat. Clim. Change 2, 186–188.

MLR (Ministry of Land and Resources of the People's Republic of China), 2004. Chinese Territory Resource Bulletin.

MLR (Ministry of Land and Resources of the People's Republic of China), 2005. Chinese Territory Resource Bulletin.

MLR (Ministry of Land and Resources of the People's Republic of China), 2006. Chinese Territory Resource Bulletin.

MLR (Ministry of Land and Resources of the People's Republic of China), 2007. Chinese Territory Resource Bulletin.

MLR (Ministry of Land and Resources of the People's Republic of China), 2008a. The Outline of National General Land Use Planning.

MLR (Ministry of Land and Resources of the People's Republic of China), 2008b. Chinese Territory Resource Bulletin.

MLR (Ministry of Land and Resources of the People's Republic of China), 2010. Chinese Territory Resource Bulletin.

Martellozzo, F., et al., 2015. Urbanization and the loss of prime farmland: a case study in the Calgary?Edmonton corridor of Alberta. Reg. Environ. Change 15 (5), 881–893.

Mathilde, C., et al., 2015. Measuring the economic impact of climatic characteristics difference on agriculture: a Ricardian analysis of farmlands in Tajikistan. Clim. Dev. 7, 454–468.

Mu, J.E., et al., 2012. Adaptation to climatic characteristics difference: changes in farmland use and stocking rate in the U. S. Mitig. adapt. strategies glob. chang. 18, 713–730.

Narges, Z., et al., 2016. Climate-induced land health risk in farmland systems: a case study of Qarasou sub-basin in Karkheh River Basin. Hum. Ecol. Risk Assess 22, 379–392.

Piao, S.L., et al., 2010. The impacts of climatic characteristics difference on water resources and agriculture in China. Nature 467, 43–51.

Pribadi, D.O., Pauleit, S., 2015. The dynamics of peri-urban agriculture during rapid urbanization of Jabodetabek Metropolitan Area. Land Use Policy 48, 13–24.

Reidsma, P., et al., 2010. Adaptation to climatic characteristics difference and climate variability in European agriculture: the importance of farm level responses. Eur. J. Agron. 32, 91–102.

Renwick, A.T., et al., 2013. Land Use Policy 30, 446–457.

Riitters, K., et al., 2009. Landscape patterns from mathematical morphology on maps with contagion. Landscape Ecol. 24, 699–709.

Solow, A.R., Smith, W.K., 2006. Using Markov chain successional models backwards. J. Appl. Ecol. 43, 185–188.

Song, W.B., et al., 2015. Urban expansion and its consumption of high-quality farmland in Beijing, China. Ecol. Indic. 54, 60–70.

Tao, F., et al., 2009. Response of crop yields to climate trends since 1980 in China. Clim. Res. 54, 233–247.

Tendall, D.M., Gaillard, G., 2015. Environmental consequences of adaptation to climatic characteristics difference in Swiss agriculture: an analysis at farm level. Agric. Syst. 132, 40–51.

Terbraak, C.J.F., Smilauer, P., 2002. CANOCO Reference Manual and User's Guide to Canoco for Windows (version 4.5). Centre for Biometry Wageningen, New York, pp. 113–180.

Vogt, P., et al., 2007. Mapping landscape corridors. Ecol. Indic. 7, 481–488.

Wang, J., et al., 2016. Risk evaluation of agricultural disaster impacts on food production in southern China by probability density method. Nat. Hazards 83, 1605–1634.

Xiong, W., et al., 2009. Future cereal production in China: the interaction of climatic characteristics difference, water availability and socio-economic scenarios. Global Environ. Change 19, 34–44.

Zhang, H., et al., 2014a. Modeling of spatial distributions of farmland density and its temporal change using geographically weighted regression model. Chin. Geogr. Sci. 24 (2), 191–204.

Zhang, Z., et al., 2014b. Spatial pattern and decadal change of agro-meteorological disasters in the main wheat production area of China during 1991–2009. J. Geogr. Sci 24, 387–396.

Zumkehr, A., Campbell, J.E., 2015. The potential for local croplands to meet US food demand. Front. Ecol. Environ. 13, 244–248.